This paper is part of the following report:

TITLE: Proceedings of the HPCMP Users Group Conference 2007. High Performance Computing Modernization Program: A Bridge to Future Defense held 18-21 June 2007 in Pittsburgh, Pennsylvania

To order the complete compilation report, use: ADA488707

Characterization of High Altitude Turbulence for Air Force Platforms

Frank H. Ruggiero
*US Air Force Research Laboratory, Space Vehicles
Directorate (AFRL/VS), Hanscom AFB, MA*
Frank.Ruggiero@hanscom.af.mil

Joe Werne
*NorthWest Research Associates, Colorado
Research Associates Division, Boulder CO*
werne@cora.nwra.com

Alex Mahalov and Basil Nichols
Arizona State University, Tempe, AZ
byn@stokes.la.asu.edu and alex@taylor.la.asu.edu

Donald E. Wroblewski
Boston University, Boston MA
dew11@bu.edu

1. Introduction

The Department of Defense (DoD) has an urgent need to both understand and predict the effects of high-altitude ($z > 10$ km) turbulence (HAT) on systems that operate at or propagate through those altitudes. Examples of systems affected by HAT include surveillance aircraft such as the U-2 and the unmanned Global Hawk, developing weapons systems such as the Airborne Laser (ABL), and developing communication systems such as the Transformational Communication Satellites (TSAT). The surveillance aircraft are primarily affected by mechanical turbulence, which is the fluctuation of wind velocity and is usually caused by velocity gradients, flow over terrain, or convection. High frequency gravity waves can affect the aircraft the same way and are caused by the same forcing mechanisms as actual mechanical turbulence and are considered as part of the HAT forecast problem. The effects of mechanical turbulence include upsetting the autopilot, degrading the quality of the surveillance observations, and in the worse case jeopardizing the aircraft itself. Laser-based systems such as the ABL and TSAT are affected by optical turbulence, which is the fluctuation of the index of refraction and is caused by mechanical turbulence in the presence of temperature gradients. For directed-energy weapon systems such as the ABL, optical turbulence causes the laser to wander, spread, and scintillate which will degrade its power, result in increased dwell time to destroy a target, and decrease the effective range. For laser-based communication systems such as TSAT, optical turbulence can result in significant data dropouts.

To address the issue of predicting high-altitude turbulence and its effects on Air Force systems, multiple DoD Challenge Projects have been carried out over the past few years to use high resolution numerical simulations to better understand turbulence that occurs in the stably stratified atmosphere above the planetary boundary layer. Specifically, two approaches have been used. First, since it is generally acknowledged that synoptic ($\Delta x \sim 100$ km) and mesoscale (1 km $< \Delta x < 100$ km) weather patterns are responsible for generating high-altitude turbulence, simulations were carried out nesting down from synoptic scale global forecast models to mesoscale models to microscale models ($\Delta x \sim O(100m)$). This allows identification and better understanding of the large scale trigger mechanisms that cause high frequency waves and turbulence at high altitudes. Second, direct numerical simulations (DNS) were conducted of limited domains to isolate the onset and evolution of turbulence for specific idealized situations, such as Kelvin-Helmholtz (K-H) instabilities. In Section 2, previous work addressing this problem will be summarized. Section 3 will briefly discuss the two codes that are currently being used to carry out the approaches discussed above. In Section 4, the results from the past year will be discussed in detail. In Section 5, the implications of the results presented here will be described.

2. Previous Work

Initial DNS of K-H instabilities by Werne and Fritts (2000) visually depicted the fact that optical turbulence and mechanical turbulence do not necessarily coincide; mechanical turbulence is large when/where mixing is large, while optical turbulence can be significantly reduced by mixing. However, optical turbulence is likely to be found on the top and bottom edges of mechanically mixed regions where the isothermal layer caused by the mixing interacts with the ambient stably stratified temperature gradient, thus enhancing the temperature variances in those areas. Early DNS results confirmed

observations of balloon measurements (Werne, et al., 2001) that show that turbulence in the free atmosphere occurs in very thin vertical layers with length scales on the order of 1 – 10 m. Werne and Fritts (2000) also computed 2nd-order structure functions for temperature and the three component winds. The results for three wind components were not close to each other, indicating that the turbulence was anisotropic, non-homogeneous and thus non-Kolmogorov. This was subsequently confirmed by aircraft observations (Wroblewski, et al., 2007).

More recent simulations Werne, et al. (2005) has expanded both the spatial and temporal domain of the K-H instabilities. This work, leveraged with Capability Application Project (CAP) grants, has allowed for the simulation of the K-H under different sub-critical Richardson numbers (Ri<0.25). This has greatly increased the understanding of the K-H process in the atmosphere. Particularly noteworthy is the striking difference in the transition to turbulence under differing stratifications. However despite the complexity of the transition to turbulence and its dependence on Ri, there are some simple laws that help us in our parameterization work. They are a) the final layer depth scales with $Ri^{-1/2}$ and b) the final Ri profile tends to 0.55.

Work with the synoptic-scale to microscale nesting started with relatively simple idealized cases such as a jet stream co-located with the tropopause (Joseph, et al., 2004) using the Arizona State University (ASU) microscale model. Results from this work showed that with fine spatial resolution in turbulent regimes, one could get good estimates of dissipation. Subsequently the approach was adapted (Mahalov, et al., 2006) and applied using the ASU microscale model nested within the Weather Research and Forecast (WRF) model. This permitted the application of the microscale code to real cases. Results from Mahalov, et al. (2006) showed the depiction of mountain waves off Greenland and the depiction of thin layers of turbulence by the microscale code that were not detected by the WRF model.

3. Methodology

The technical approach employed for the high-resolution simulations of atmospheric wind shears uses the DNS code named TRIPLE which is an incompressible pseudo-spectral Navier-Stokes solver that uses Fourier and Chebyshev spatial discretizations. It is a mature production code that has served as the workhorse for six DoD High Performance Computing Modernization Program (HPCMP) and NSF Grand Challenge projects and two HPCMP CAP Phase II projects. The numerical method advances the Fourier and/or Chebyshev coefficients in spectral space. Potential truncation errors

are removed using the "tau"-correction (Werne, 1995), and vertical stacking of Chebyshev domains is possible. The method is Nth-order accurate in space, where N is the number of spectral modes. Depending on the application (i.e., wave-breaking, shear, convection, etc.), different spatial representations are used. Possible boundary conditions include stress-free, no-slip, fixed-temperature or heat-flux, radiative, incident gravity waves, or any combination thereof. For shear-instability and reduced-equation studies, greater computation speeds are achieved by employing simpler boundary conditions permitted by these problems. For these cases stress-free top and bottom boundaries permit Fourier representations in the vertical, and complicated inversion operations can be avoided.

Time-stepping is conducted using the mixed implicit/explicit 3rd-order Runge-Kutta (RK3) scheme of Spalart, et al. (1991), which has the same storage requirements of most 2nd-order schemes, allowing us to achieve larger numerical domains than would otherwise be possible. Nonlinear terms are treated explicitly, while buoyancy and diffusion are handled implicitly. Derivatives (non-linear terms) are computed efficiently in spectral (physical) space.

Initial wind-shear solutions (i.e., Werne and Fritts, 2000) were computed in domains of size $(\lambda, \lambda/3, 2\lambda)$ in the (streamwise, spanwise, vertical) directions, where λ is the wavelength of the most unstable asymptotic linear eigen mode for the K-H instability. In the initial period of this Challenge project and with additional resources from the 2004 CAP II allocations, expanded runs were completed in domains of size $(4\lambda, 2\lambda, 2\lambda)$, for the Ri of 0.05, 0.15, and 0.20 and Reynold's number (Re) of 2500 (Werne et al., 2005). In the past year and again with the help of additional resources from the 2006 CAP II program, the 0.15 and 0.20 were rerun with Re of 2,900 and 4,000 respectively. These Re were chosen so that all solutions required nearly the same number of spectral modes, which peaked at (nx, ny, nz) = (3,600, 1,800, 1,800).

For the meso to mircoscale portion of this work the Advanced Research WRF core (Skamarock et al., 2005) was used. The model uses a time-split integration scheme where low-frequency modes that are meteorologically significant are integrated using a RK3 time integration scheme and high-frequency acoustic modes are integrated implicitly in the vertical over smaller time steps to maintain stability. Spatial discretization is done using a C grid staggering where normal velocity are staggered one-half grid length from the thermodynamic variables. Advection of vector and scalar fields is in the form of flux divergence, and is performed using the third order Runge-Kutta time-integration scheme using a fifth- and third-order accurate spatial discretization.

The WRF model was run for a case during the 2005 Terrain-induced Rotors Experiment (T-REX). The standard WRF model was configured with three nests. The outermost nest received its initial and lateral boundary conditions from the European Centre for Medium-range Weather Forecasting's (ECMWF) global forecast model which provides data at a horizontal resolution of 25 km and 91 vertical levels up to 0.1 hPa. The three nested WRF grids had horizontal resolutions of 15, 3, and 1 km for each succeeding inner-nest and 150 vertical levels up to 10 hPa. Within the third nest a fourth, microscale, nest is employed. Instead of using the previous Arizona State University (ASU) microscale code, a new code has been developed, based on the full WRF equations, algorithms and subroutines. This WRF compatible code runs in a one-way nesting with WRF and allows for both horizontal and vertical nesting. Both upper vertical and lateral boundary conditions are relaxed to the fields of the finest third WRF nest, including the vertical velocity. Following microscale algorithms from previous ASU codes, an adaptive staggered mesh is implemented in the vertical, with a denser grid around the tropopause and in the lower stratosphere. The new WRF-like code was run with a horizontal resolution of 333 m and with 720 vertical levels.

4. Results

A. K-H Wind Shear Simulations

Results from the higher Re runs show fuller spectra and more complete turbulence statistics than the previous runs. The comparisons of the DNS with aircraft observations begun last year (Ruggiero, et al., 2006) has continued and has gone beyond the validation of the DNS results. Analysis of high frequency aircraft measurements by Wroblewski, et al. (2007) has detailed distinct signatures in the plots of temperature and winds observed along the aircraft's flight path. These plots have been compared to simulated transects through the K-H simulations. Of particular interest is to compare the different signatures within the transects and identify particular signatures or fingerprints that are indicative of a particular initial Ri number and temporal point in the turbulence evolution. Figure 1 is a comparison of the DNS and aircraft data. Both plots exhibit the classic cliff-ramp structure in the potential temperature traces. The presence of the relatively smoothed ramps without steps indicates that the aircraft measurements occurred in the latter stages of the cliff-ramp evolution. Another comparison shown in Figure 2 shows the combination of cliff-steps and cliff ramps that suggest either an early time for Ri=0.20 or late time for Ri=0.15. Ultimately the Ri =0.15 scenario was chosen as the best match because of

the lack of cliffs in the U wind field. The real intriguing point of these results is how given a set of meteorological variables (in this case high-resolution temperature and wind data), one can gain additional information such as initial Ri and age of the turbulence layer by comparing directly with DNS results.

B. Microscale Nesting

The microscale case study highlighted here is from the TREx Intensive Observation Period (IOP) 8 that took place on 31 March–1 April in the Owens Valley region of California. The primary focus of the experiment was to explore the structure and evolution of atmospheric rotors (intense low-level horizontal vortices that form on axis parallel to, and downstream of, a mountain ridge crest) as well as associated phenomena in complex terrain. As such it provides an excellent case to study the generation of mountains waves and its associated turbulence at high altitudes. For this case the WRF model with the custom WRF microscale nest was initialized on 31 March 2006 at 00 UTC. Figure 3 shows a cross section Richardson's number and the square of the wind shear across the Owens Valley from the microscale nest valid on 1 April 2006 at 08 UTC. Clearly flow coming over the over mountains from the west is causing increased shear and turbulence in the valley itself. But what is interesting to note is that above the approximate height of the Sierra Nevada mountains to the west of the valley, the atmosphere is relatively stable up to 10–15 km at which point turbulence layers (Ri < 0.25) are noted beginning in horizontal near the peak of the Sierra Nevada ridge and continuing down wind. Evidence of the turbulence layers above 10 km on the microscale nest is confirmed by coincident radiosonde data (not shown). The temperature profile indicates wave activity occurring above the tropopause (located at approximately 10.5 km MSL) along with enhanced wind shear. Estimations of vertical velocity based on the rise rate of the balloon show vertical velocities exceeding 7 m/s at several altitudes above the tropopause. These values for vertical velocity would have a substantial impact on aircraft operating at these altitudes.

5. Significance to DoD

The goal of this project is to improve prediction of high-altitude turbulence and quantify its effects on DoD systems. Currently the microscale nesting work is achieving the latter by providing high resolution characterization of the atmosphere, including turbulence, in support of testing of the Airborne Laser that has begun this spring. Immediately after a laser test, the WRF model with microscale nesting is run. The results from

the microscale nest are used to explicitly calculate turbulence parameters such as the Ri and the refractive index structure constant, a measure of optical turbulence. Using these variables, ABL testers can characterize the atmosphere they are lasing through and predict future test results and operational capabilities.

In the DNS results described above it was demonstrated that given a certain set of atmospheric variables, in this case temperature and winds along a flight path, and comparing them to DNS one can extract additional information about the atmosphere, such as Ri and the age of the turbulence evolution. This leads to an opportunity to infer the subgrid-scale turbulence fields by comparisons with DNS results once a set of meteorological variables are obtained from an operational mesoscale model. This is possible because of progress in recent years in applying Bayesian Hierarchical Modeling (BHM) techniques to geophysical applications where the character of BHM is particularly well suited to addressing measurement and model uncertainty, while quantitatively incorporating significant scientific understanding. An additional advantage of the BHM approach is that it produces a probabilistic forecast which is more realistic for solving the problem since mesoscale models cannot explicitly resolve the turbulent flow and are therefore unable to make a deterministic forecast. Currently the DNS results along with the aircraft data cited above and balloon measurements will be used to relate conditional probabilities of the occurrence of optical turbulence based on input from operational mesoscale models to produce the next generation of optical turbulence prediction for the ABL.

Acknowledgments

References

Joseph B., A. Mahalov, B. Nicolaenko, and K. L. Tse, "Variability of turbulence and its outer scales in a nonuniformly stratified tropopause jet." *J. Atmos. Sci.*, 41, pp. 524–537, 2004.

Mahalov, A., M. Moustaoui, and B. Nichols, "Characterization and forecasting of stratospheric Clear Air Turbulence (CAT) for Air Force Platforms." *Proceedings, HPCMP Users Group Conference 2006*, Denver, CO, 26–29 June, pp. 288–293, 2006.

Ruggiero, F.H., J.A. Werne, A. Mahalov, and B. Nichols,:"Characterization of High Altitude Turbulence for Air

Force Platforms." *Proceedings of the HMCMP Users Group Conference 2006*, Denver, CO, 26–29 June 2006, pp. 296–300, 2006.

Skamarock, W.C., J.B. Klemp, J. Dudhia, D.O. Gill, D.M. Barker, W. Wang, and J.G. Powers, "A Description of the Advanced Research WRF Version 2." *NCAR Tech. Note, NCAR/TN-468+STR* 98, 2005, http://www.mmm.ucar.edu/wrf/users/docs/arw_v2.pdf.

Spalart, P.R., R.D. Moser, and M.M. Rogers, "Spectral methods for the Navier-Stokes equations with one infinite and two periodic directions." *J. Comput. Phys.*, 96, pp. 297–324, 1991.

Werne, J., "Incompressibility and no-slip boundaries in the Chebyshev-Tau approximation: Correction to Kleiser and Schumanns influence-matrix solution." *J. Comput. Phys.*, 120, pp. 260–265, 1995.

Werne, J. and D.C. Fritts, "Structure functions in stratified shear turbulence." *Proceedings HPCMO Users Group Conference 2000*, Albuquerque, NM, 5–8 June, 2000.

Werne, J., T. Lund, D. Fritts, B.A. Pettersson-Reif, and P. Sullivan, "CAP Phase II simulations for Air Force HEL-JTO Project: Atmospheric turbulence simulations on NAVO's 3000-processor IBM P4+ and ARL's 2000-processor Intel Xeon EM64T cluster." *Proceedings of the HMCMP Users Group Conference 2005*, Nashville, TN, 27–30 June 2005, pp. 100–111, 2005.

Werne, J. C. Bizon, CMeyer, and D. Fritts, "Wave breaking and shear turbulence simulations in support of the Airborne Laser." *Proceedings, HPCMP Users Group Conference 2001*, Biloxi, MS, 18–22 June, 2001.

Wroblewski, D., O.R. Coté, J.M. Hacker, R.J. Dobosy, "Cliff-ramp patterns and Kelvin-Helmholtz billows in stably stratified shear flow in the upper troposphere: Analysis of aircraft measurements." *J. Atmos. Sci.*, 2007 (in press).
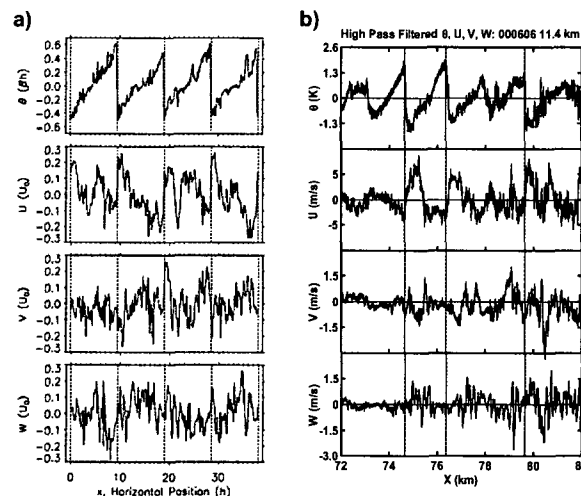
Figure 1. Transects of potential temperature and the u, v, and w wind components for (a) K-H DNS with Ri = 0.2 and non-dimensional time τ = 77 and (b) aircraft flights over Wales, UK 6 June 2000. For the DNS plots the temperature is scaled by the product of vertical potential temperature gradient and distance from the center of the billow and the winds are scaled by the mean horizontal wind speed.
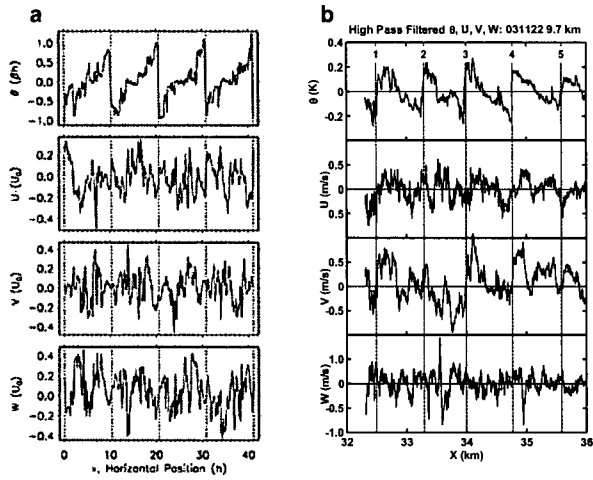
Figure 2. Transects of potential temperature and the u, v, and w wind components for (a) K-H DNS with Ri = 0.15 and non-dimensional time τ = 72.6 and (b) aircraft flights north of Darwin, Australia on 22 November 2003. Scaling for the DNS plots is the same as for Figure 1.
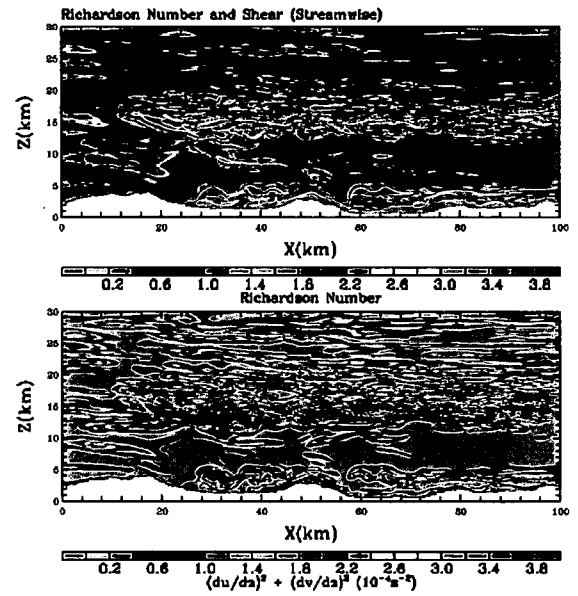

Figure 3. Upper panel: (118.56W, 117.42W)-altitude cross-section at latitude 36.82N for Ri Lower: Cross-section for the square of the shear field for the innermost microscale domain (333m grid). Both plot valid for 8:00 UTC, April 1, 2006.